The Korean Journal of Ceramics, 1 [4] 179-184 (1995)

Phase Distribution, Microstructure, and Electrical Characteristics of NASICON Compounds

N.-H. Cho, Hee-Bok Kang*, and Y.H. Kim*

Dept. of Ceram. Eng., Inha Univ., 253 Yonghyun-dong, Nam-ku, Incheon 402-751, Korea
**Division of Ceram., Korea Institute of Sci. and Tech., P.O. Box 131, Cheongryang, Seoul 130-650, Korea*
(Received November 8, 1995)

Sodium superionic conductor (NASICON) compounds were prepared. The effects of sintering temperature and cooling rate on the formation and the distribution of crystalline NASICON and ZrO_2 second phase were investigated. In the von Alpen-type composition, the ZrO_2 second phase is in thermal equilibrium with the crystalline NASICON above 1320°C, but when cooled through 1260-1320°C crystalline NASICON was formed by reaction between ZrO_2 and liquid phase. Very slow cooling (1°C/hr) to 1260°C from sintering temperature decreased the amount of sodium which prevents the formation of the crystalline NASICON resulted high number of ZrO_2 grains near the surface of some sintered bodies. Maximum electrical conductivity of 0.200 $ohm^{-1}cm^{-1}$ was obtained at 300°C for well-sintered samples with little ZrO_2. On the other hand, low conductivities were obtained for rapid-cooled samples which have less dense microstructure.

Key words : NASICON, ZrO_2 second phase, Von Alpen-type, Microstructure, Electrical conductivity

I. Introduction

Sodium superionic conductor (NASICON) with a chemical formular of $Na_{1+x}Zr_2Si_xP_{3-x}O_{12}$ was first reported by Hong et al as solid electrolyte materials.[1,2] The compound has been investigated intensively over the last decade mainly due to its promising electrical properties suitable for gas sensor and energy storage systems.[3-6]

NASICON has some useful and unique characteristics such as low sintering temperature, three dimensional framework, and considerably good ionic conductivity compared to other solid electrolytes particularly β-alumina.[7-9] Though β-alumina has attracted much attention for the application in the Na-S battery system,[10-12] it has a layer structure with undesirable directionality in thermal expansion and electrical flows.[13] On the other hand, NASICON has been reported to exhibit a few crystalline forms depending on temperature and composition (x), and most sintered NASICON contain certain amount of ZrO_2 second phases. Unfortunately, the ZrO_2 has a monoclinic/tetragonal phase transition at 1100°C, below the usual sintering temperatures of the NASICON compounds. In addition, the monoclinic/rhombohedral phase transition of crystalline NASICON around 200°C causes dilatometric anomaly unfavorable for industrial applications.[14-15]

To overcome such technical problems, we have investigated about the phases, such as ZrO_2 and crystalline NASICON present in von Alpen-type NASICON. The von Alpen-type NASICON is of a ZrO_2 deficient form of the Hong's NASICON with a general formular of $Na_{1+x}Zr_{2-x/3}Si_xP_{3-x}O_{12-2x/3}$, containing little ZrO_2 second phase.[14] In this study, the von Alpen-type NASICON was used mainly because we could obtain some kinetic informations about phase transformation due to the absence of ZrO_2 second phase in sintered NASICON. The effects of sintering temperature and cooling rate on the formation and the distribution of the ZrO_2 and the crystalline NASICON were investigated. The electrical characteristics of the sintered NASICON was examined and correlated with their microstructures.

II. Experimental

Starting materials used in the preparation of the NASICON compounds were highly pure powders of Na_2CO_3, $Na_3PO_412H_2O$, ZrO_2, and SiO_2. These materials were dried at 120°C for 12 hours and then mixed according to the stoichiometric ratio of $Na_{3.1}Zr_{1.55}Si_{2.3}P_{0.7}O_{11}$. The mixtures were calcined at 1150°C for 10 hours. The calcined powders were ball milled in ethanol media using zirconia balls for 30 hours and dried. The powders were pressed into tablets under a pressure of 1000 kg/cm^2.

Various sintering temperatures and cooling paths were chosen to investigate the formation and the distribution of the ZrO_2 and the crystalline NASICON. The tablets were sintered from 1200°C to 1360°C for 1 hour. Fig. 1 shows the various sintering and cooling schedules.

Phases present in the sintered samples were identified by X-ray diffraction (XRD, Philips, ADP 1700) using CuKα radiation with Ni filter. Microstructure and chemical composition change were analyzed by scanning elec-

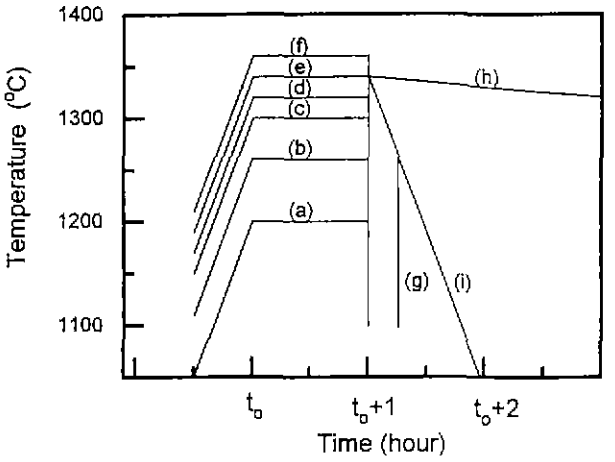

Fig. 1. Sintering temperatures and cooling paths for the investigated samples. The samples were sintered at (a) 1200°C, (b) 1260°C, (c) 1300°C, (d) 1320°C, (e) 1340°C , and (f) 1360°C for 1 hour respectively, followed by air quench. Some samples were sintered at 1340°C for 1 hour and then either (g) furnace-cooled to 1260°C or (h) cooled at 1°C/hr to 1260°C, followed by air quench. Cooling path (i) indicates furnace-cooling to room temperature after sintering at 1340°C for 1 hour. The furnace-cooling rate is about 5°C/min.

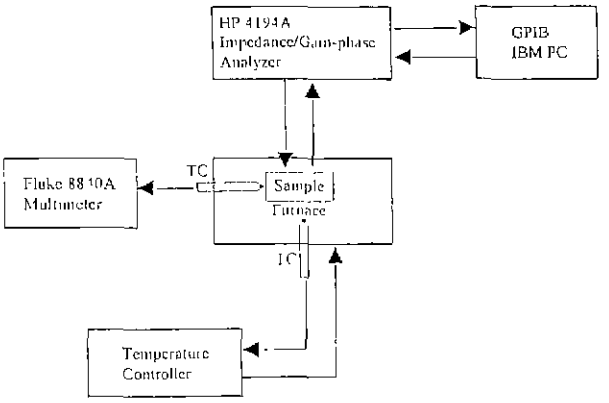

Fig. 2. Schematic representation for the conductivity measurement system.

tron microscopy (SEM, Hitachi, X-650) with an energy dispersive spectrometry (EDS) system. In the EDS investigation, an electron beam of about 10nm diameter was used. The variation in the amount of sodium depending on position was estimated by comparing the ratio of the peak height of Na Kα to the peak height of Si Kα: the EDS information was obtained by scanning a certain area at the corresponding position with an electron beam.

To measure electrical conductivity, the flat surfaces of the tablets were prepared by polishing with successively fine grades of Al_2O_3 powder followed by diamond pastes down to 1 μm. Silver pasted on the flat surfaces was used as electrode materials. Conductivities were measured with an Impedance/gain-phase analyzer (HP 4194A) in a frequency range of 10^2 to 4×10^6 Hz from room temperature to 300°C. A simple electrically heated furnace was employed: nitrogen gas was circulated inside the furnace and the temperature was measured with chromel-alumel thermocouples in contact with the electrode. Schematic representation of the measurement system is shown in Fig. 2.

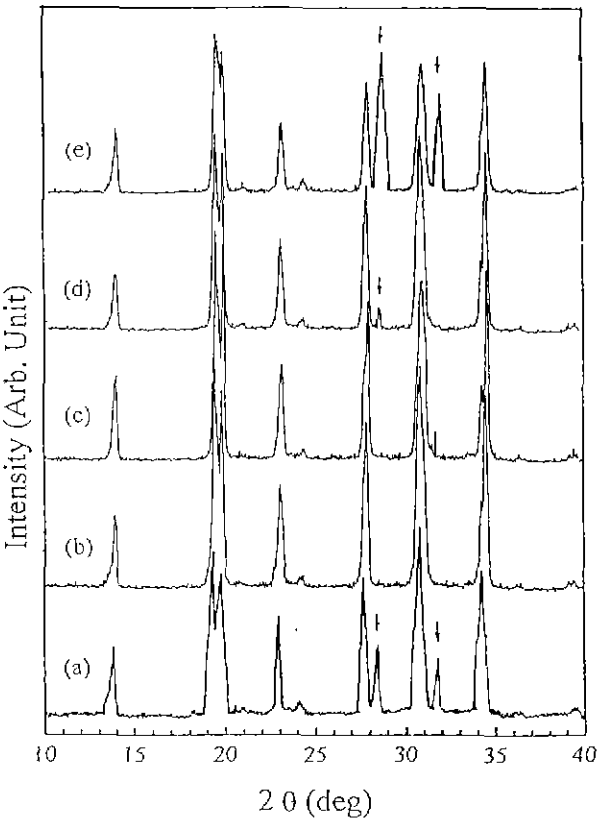

Fig. 3. XRD patterns of the air quenched samples. These samples were sintered for 1 hour at (a) 1200°C, (b) 1260°C, (c) 1300°C, (d) 1320°C, and (e) 1360°C, respectively. Arrows indicate ZrO_2 peaks

III. Results and Discussions

1. Effects of sintering temperature and cooling rate on phase distribution

Fig. 3 shows the XRD curves of the samples sintered at 1200°, 1260°, 1300°, 1320° and 1360°C for 1 hour respectively and then air-quenched to room temperature. All the peaks correspond to either monoclinic NASICON or ZrO_2: the ZrO_2 peaks are indicated with arrows. Spectra (b) and (c) consist of only the crystalline NASICON. However, as seen in spectra (d) and (e), the samples sintered above 1320°C contain ZrO_2 second phase peak. As all the samples were made by air quench after sintering, it is believed that considerable amounts of ZrO_2 is in thermal equilibrium with the crystalline NASICON at 1340°C (Fig. 4b).

In order to investigate the existence of the ZrO_2 phase when cooled through 1260-1300°C, two different cooling

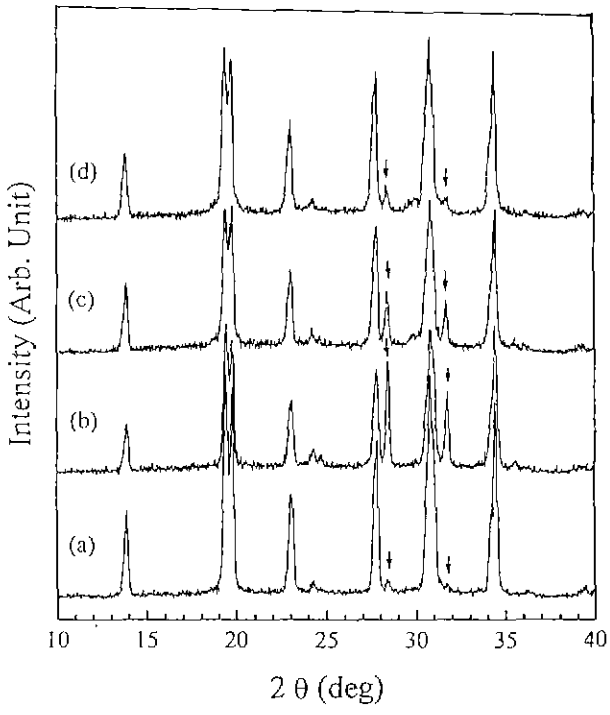

Fig. 4. XRD patterns of the samples sintered at 1340°C for 1 hour. These samples were (a) furnace-cooled to room temperature, (b) air quenched to room temperature, (c) cooled to 1260°C at 1°C/hr followed by air quench, and (d) furnace-cooled to 1260°C followed by air quench, respectively.

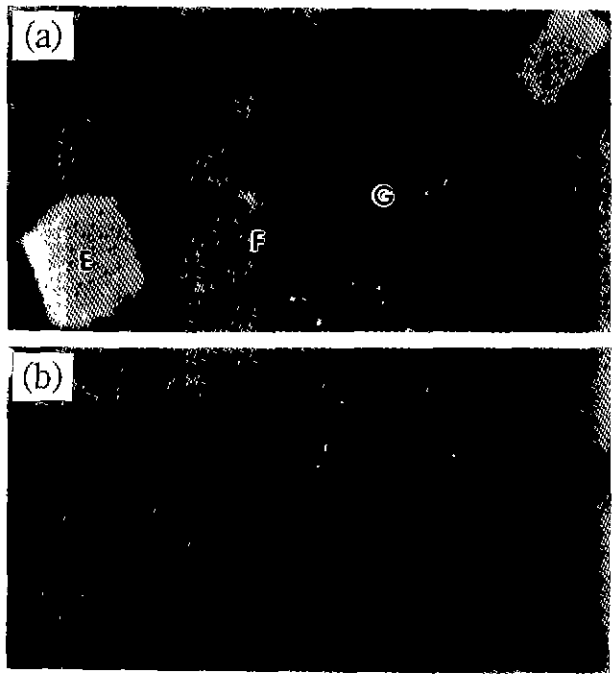

Fig. 5. Scanning electron micrographs. The samples were sintered at 1340°C for 1 hr, and then (a) air quenched and (b) furnace-cooled to room temperature respectively. In micrograph (a), bright (E), grey (F), and dark (G) regions correspond to the ZrO_2, crystalline NASICON, and glass phases, respectively.

paths were employed:

First, in samples sintered at 1340°C for 1 hour and then furnace-cooled to 1260°C, followed by air quench to room temperature (Fig. 4d), the amount of ZrO_2 second phase decreases significantly. This indicates that a peritectic type reaction between the crystalline NASICON and the ZrO_2 occured around 1320°C as shown in the reaction equation below.

$$ZrO_2 + \text{liquid phase} \underset{\text{heating}}{\overset{\text{cooling}}{\rightleftharpoons}} \text{NASICON}$$

Second, in samples sintered at 1340°C for 1 hour and then cooled to 1260°C very slowly (at 1°C/hr), followed by air quench to room temperature (Fig. 4c), considerable amounts of ZrO_2 second phase was present. The explanation to this unexpected amount of ZrO_2 second phase is given in the next section.

2. Microstructural changes during sintering

The SEM micrographs of the samples air-quenched and furnace-cooled from 1340°C to room temperature, respectively, are shown in Fig. 5. The general microstructure of the sintered NASICON has been described earlier.[15,18] The bright, grey, and dark regions in Fig. 5(a) can be attributed to ZrO_2, crystalline NASICON, and glass phases, respectively. On the other hand, as shown in Fig. 5(b), no ZrO_2 is present in the furnace-cooled samples. This seems to be in good agreement with XRD results in Fig. 4(a).

The crystalline NASICON present in the air-quenched samples exhibit a considerably sharp interface with the liquid phase, whereas in the furnace-cooled samples the interface between the crystalline phase and the liquid phase is less clearly seen. During the furnace-cooling process, the ZrO_2 phase, stable at 1340°C, interacts with the liquid phase to produce the crystalline NASICON. The amount of the crystalline NASICON increased at the expense of the liquid phase during the furnace-cooling process, and thereafter the bulk density of the materials would increase, affecting the electrical properties of the sintered bodies.

Fig. 6(a) shows a cross-section view of the samples which were sintered at 1340°C for 1 hour and then cooled to 1260°C at 1°C/hr, followed by air quench. The number of ZrO_2 grains is very high in the region between two bars indicated by t near the surface. On the other hand, there is no contrast for the presence of ZrO_2 grains near the surface of the samples which were furnace-cooled to room temperature from the sintering temperature (Fig. 6(c)). EDS results were obtained from a rectangular shape area (200 μm × 20 μm) in the region indicated by t in Fig. 6(a), and an inner region of the sample, respectively. These spectra are shown in Fig. 7. The amount of sodium near the surface region was less than that of the inner region. Consequently no crystalline NASICON could form in the surface region.

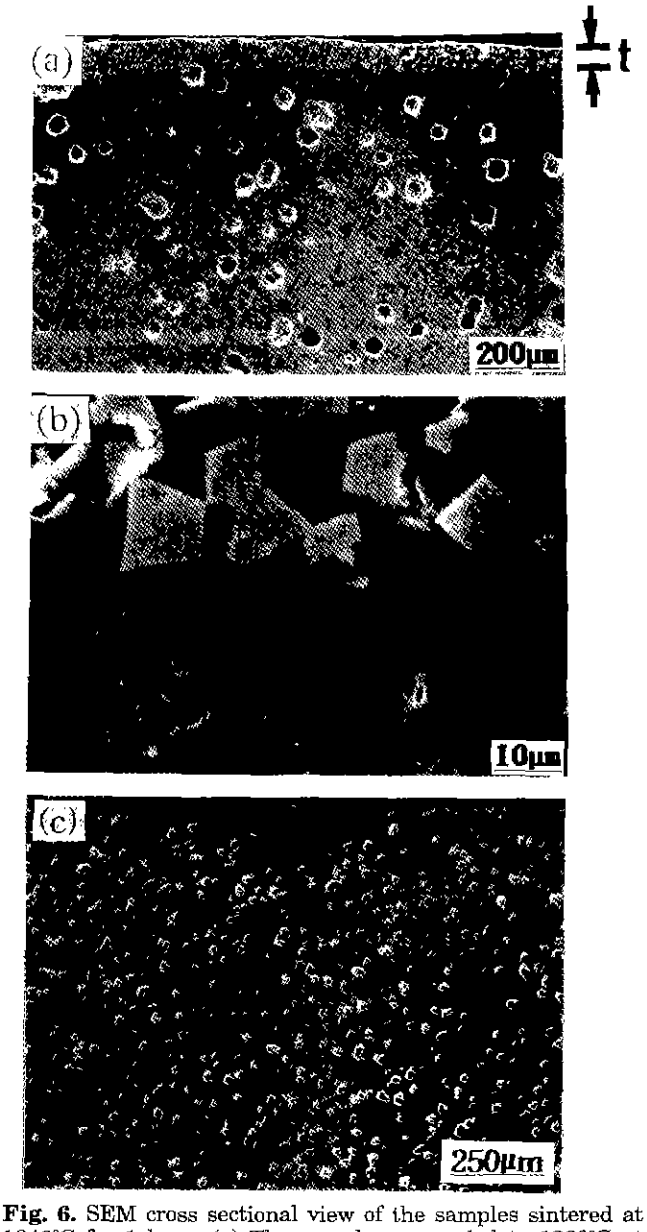

Fig. 6. SEM cross sectional view of the samples sintered at 1340°C for 1 hour. (a) The sample was cooled to 1260°C at 1°C/hr followed by air quench; many ZrO_2 grains are seen in the region between two bars indicated by t near the surface. (b) An enlargement of the surface area of (a). (c) The sample was furnace-cooled to room temperature.

In cooling below the congruent point, the amount of ZrO_2 second phase would decrease with time because the phase is unstable thermodynamically. Therefore, slow-cooling through 1260-1320°C would be favorable to minimize the amount of ZrO_2 second phase in sintered NASICON. But increasing cooling time through the temperature range resulted the decrease in the amount of sodium in the sintered bodies. This appeared to occur mainly near the surface region. Such a deviation in composition from that of the starting materials prevents the formation of crystalline NASICON. This indicates that cooling rate should not be too slow to lose sodium near

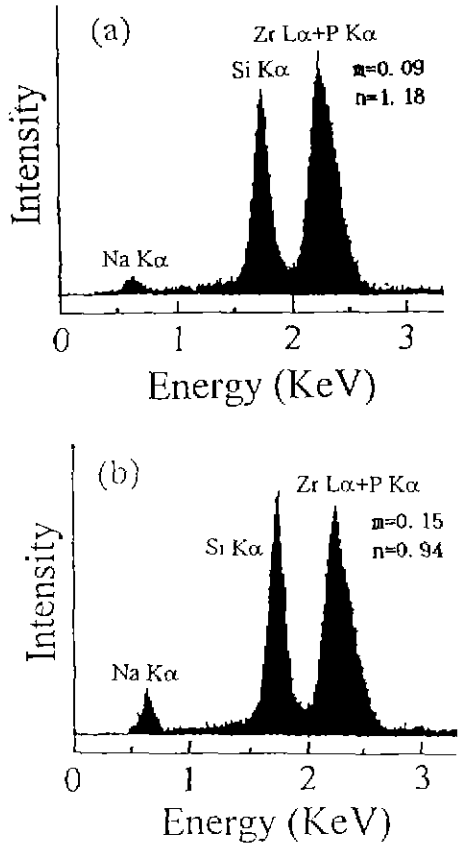

Fig. 7. Energy dispersive spectra for the samples shown in Fig. 6. Spectra (a) and (b) were obtained from a rectangular-shaped area (20 μm × 200 μm) near the surface and inner region, respectively. Letters m and n denote the ratios of Na Kα/Si Kα, and Zr Lα/Si Kα, respectively.

surface excessively.

3. *Electrical characteristics*

A frequency range of 10^2 to 4×10^6 Hz was used to measure the ionic conductivity of the sintered NASICON. The dc conductivity of the samples prepared through three different cooling paths from 1340°C were investigated. Fig. 8 shows the conductivity(σ)-frequency(f) relation of the sample which was sintered at 1340°C for 1 hour and furnace-cooled to room temperature. The dc conductivity was taken as the value of the frequency independent plateau in the σ-f plot.[19,20] At various conductivity measuring temperatures between room temperature and 300°C in this investigation, a part of this plateau was observed within the range of experimental frequencies, and dc conductivities at each temperature could be determined from relevant plots. In Fig. 8, frequency independent regions are clearly seen in each curve obtained at temperatures from 40°C to 300°C. The measured conductivities were ploted over a wide temperatrue range so that Arrhenius equation could be applicable (Fig. 9).

The samples which were furnace-cooled exhibit much

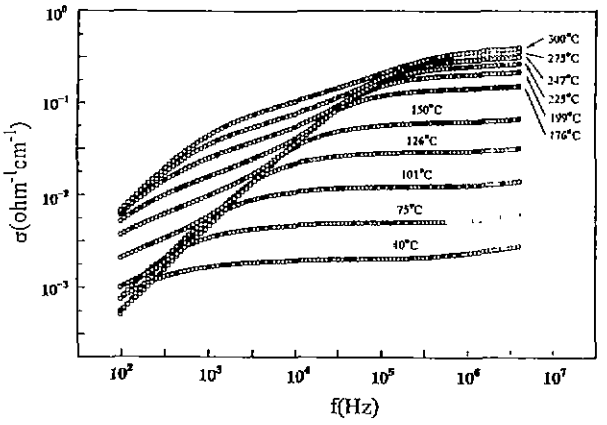

Fig. 8. Electrical conductivities for the sintered NASICON. A systematic change in the positions of frequency-independent region is observed with increasing measurement temperature.

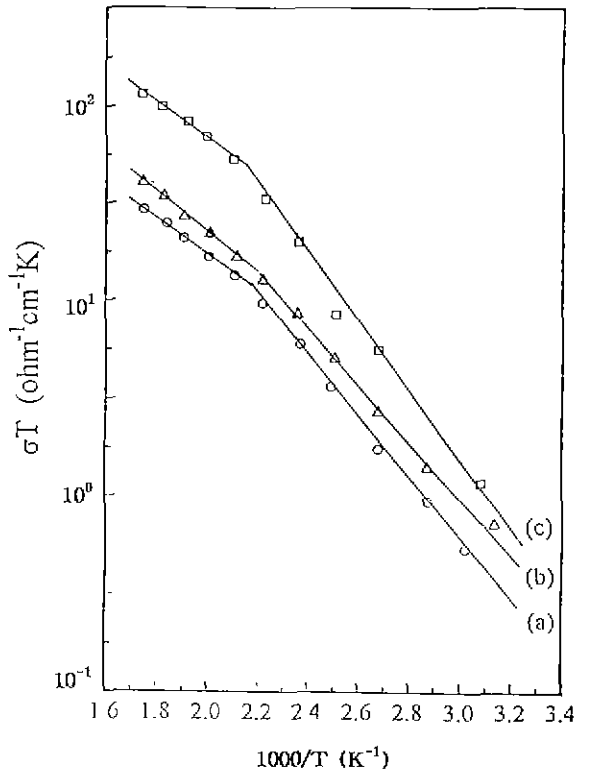

Fig. 9. σT vs. 1000/T for the sintered NASICON. Curves (a), (b), and (c) were obtained from the samples sintered at 1340°C for 1 hour, and then air quenched, furnace-cooled to 1250°C followed by air quench, and furnce-cooled to room temperature, respectively.

higher conductivity than the other two types of samples in Fig. 9. In particular, at 300°C maximum conductivity of 0.200 $ohm^{-1}cm^{-1}$ was measured, which is comparable to the conductivity of polycrystalline β″-alumina reported by Virkar and Hooper.[10] The conductivities seem to fit the Arrhenius equation over the sintering temperature range. At temperatures of around 200°C, a significant change in activation energy occurs for all the three different types of samples, corresponding to the NASICON monoclinic/rhombohedral transition. In the higher temperature region, three curves (a), (b), and (c) exhibit a similar activation energy of about 0.09 eV, but the microstructural differences caused by various cooling paths appears to result in the conductivity differences among the three curves ($0.14 < \sigma < 0.2$ $ohm^{-1}cm^{-1}$ at 300°C). On the other hand, in the lower temperature region, an activation energy of about 0.13 eV was measured. The conduction barrier height is affected by the polymorphism of the crystalline NASICON, and denser sintered NASICON is favorable for higher electrical conductivity.

IV. Conclusion

An appropriate choice of sintering temperature and cooling rate is essential in producing sintered NASICON with less ZrO_2 and higher electrical conductivities. In our investigation, a particular temperature region was found in which no ZrO_2 exist in the sintered bodies as a thermodynamically stable phase. The NASICON compounds sintered above the congruent point should be cooled slow through 1260-1300°C so that the ZrO_2 second phase could be completely dissolved into the crystalline NASICON. However, cooling rate should not be too slow to lose sodium near surface excessively. As was expected, denser sintered bodies are favorable for higher electrical conductivity. Maximum conductivity of 0.2 $ohm^{-1}cm^{-1}$ was obtained at 300°C for the sintered NASICON with little ZrO_2 second phase.

Acknowledgement

The authors acknowledge the financial support for this work by Inha University (1994).

References

1. H. Y-P. Hong, "Crystal Structures and Crystal Chemistry in the System $Na_{1+x}Zr_2Si_xP_{3-x}O_{12}$," *Mat. Res. Bull.*, **11**, 173-182 (1976).
2. J. B Goodenough, H. Y-P. Hong, and J. A. Kafalas, "Fast Na^+ ion Transport in Skeleton Structure," *Mat. Res. Bull.*, **11**, 203-220 (1976).
3. R. S. Gordon, G. R. Miller, T. D. Hadnagy, B. J. McEntire, and T. R. Rasmussen, "Ceramics in High Performed Batteries," pp. 925-949 in Energy and Ceramics, Edited by P. Vincenzini, Elsevier, New York, 1980.
4. T. Maruyama, Y. Saito, Y. Matsumoto, and Y. Yano, "Potentiometric Sensor for Sulfur Oxides Using Nasicon as a Solid Electrolyte," *Solid State Ion.*, **17**, 281-286 (1985).
5. D. Ravaine, and J. L Souquet, "Ionic Conductive Glasses," pp. 277-290 in Solid Electrolytes, Edited by P. Hagenmuller and W. Van Gool, Academic Press, New York, 1978.
6. Y. Saito, T. Maruyama, and S. Sasaki, "Gas Sensors Using Nasicon as a Solid Electrolyte," Report of the

Research laboratory of Engineering Materials, Tokyo Institute of Technology, **9**, 17-26 (1984).

7. S. Fujitsu, M. Nagai, and T. Kanazawa, "Conduction Paths in Sintered Ionic Conductive Material $Na_{1+x}Y_xZr_{2-x}(PO_4)_3$," *Mat. Res. Bull.*, **16**, 1299-1309 (1981).
8. P. G. Komorowski, S. A. Argyropoulos, J. D. Canaday, A. K. Kuriakose, T. A. Wheat, A. Ahmad, and J. Gulens, "The Study of Hydronium Nasicon Conductivity with Deuterium," *Solid State Ion.*, **50**, 253-258 (1992).
9. O. Tillement, J. Angenault, J. C. Conturier, and M. Quarton, "Electrochemical Studies of Mixed Valence Nasicon," *Solid State Ion.*, **53**, 391-399 (1992).
10. P. T. Moseley, "The Solid Electrolyte-properties and Characteristics," pp. 19-77 in the Sodium Sulfer Battery, Edited by J. L. Sudworth and A. R. Tilley, Champman and Hall, New York, 1985.
11. S. Yamaguchi, and A. Imai, "Review on Sodium ion Conductors and Their Applications," *Ceramics Japan*, **27**[2], 122-127 (1992).
12. B. J. McEntire, G. R. Miller, and R. S. Gordon, "Sintering of Polycrystalline Ionic Conductors: β''-Al_2O_3 and Nasicon," pp. 517-524 in sintering process, Edited by Kuczynski, Plenum Press, New York, 1980.
13. B. J. McEntire, R. A. Bartlett, G. R. Miller, and R. S. Gordon, "Effect of Decomposition on the Densification and Properties of Nasicon Ceramic Electrolytes," *J. Am. Ceram. Soc.*, **66**[10]. 738-742 (1983).
14. U. Von Alpen, M. F. Bell, and H. H. Hofer, "Compositional Dependence of the Electrochemical and Structural Parameters in the Nasicon System $(Na_{1+x}Si_xZr_2P_{3-x}O_{12})$," *Solid State Ion.*, **3/4**, 215-218 (1981).
15. A. K. Kuriakose, T. A. Wheat, A. Ahmad, and J. Dirocco, "Synthesis, Sintering and Microstructure of Nasicons," *J. Am. Cer. Soc.*, **67**[3]. 179-183 (1984).
16. R. S. Gordon, G. R. Miller, B. J. McEntire, E. D. Beck, and J. R. Rasmussen, "Fabrication and Characterization of Nasicon Electrolytes," *Solid State Ion.*, **3/4**, 243-248 (1981).
17. A. Ahmad, T. A. Wheat, A. K. Kuriakose, J. D. Canaday, and A. G. McDonald, "Dependence of the Properties of Nasicons on Their Composition and Processing," **24**, 89-97 (1987).
18. J. J. Kim, T. S. Oh, M. S. Lee, J. G. Park, and Y. H. Kim, "Effects of Al_2O_3 Addition on the Sinterability and Ionic Conductivity of Nasicon," *J. Mat. Sci.*, **28**, 1573-1577 (1993).
19. I. M. Hodge, M. D. Ingram, and A. R. West, "Ionic Conductivity of Li_4SiO_4, Li_4GeO_4, and Their Solid Solutions," *J. Am. Ceram. Soc.*, **59**, 360-366 (1976).
20. R. J. Grant, I M. Hodge, M. D. Ingram, and A. R. West, "Migration Losses in Single Crystal Ionic Conductors: Sodium Beta Alumina and $LiGaO_2$," *J. Am. Ceram. Soc.*, **60**, 226-229 (1977).